

Efficient proximal gradient algorithms for joint graphical lasso

Jie Chen¹, Ryosuke Shimmura¹, and Joe Suzuki¹

¹Graduate School of Engineering Science, Osaka University, Japan.

Abstract

We consider learning an undirected graphical model from sparse data. While several efficient algorithms have been proposed for graphical lasso (GL), the alternating direction method of multipliers (ADMM) is the main approach taken concerning for joint graphical lasso (JGL). We propose proximal gradient procedures with and without a backtracking option for the JGL. These procedures are first-order and relatively simple, and the subproblems are solved efficiently in closed form. We further show the boundedness for the solution of the JGL problem and the iterations in the algorithms. The numerical results indicate that the proposed algorithms can achieve high accuracy and precision, and their efficiency is competitive with state-of-the-art algorithms.

1 Introduction

Graphical models are widely used to describe the relationships among interacting objects [Lauritzen, 1996]. Such models have been extensively used in various domains, such as bioinformatics, text mining, and social networks. The Graph provides a visual way to understand the joint distribution of an entire set of variables.

In this paper, we consider learning Gaussian graphical models that are expressed by undirected graphs. It represents the relationship among continuous variables that follow a joint Gaussian distribution. In an undirected graph $\mathcal{G} = (V, E)$, edge set E represents the conditional dependencies among the variables in vertex set V .

Let X_1, \dots, X_p ($p \geq 1$) be Gaussian variables with covariance matrix $\Sigma \in \mathbb{R}^{p \times p}$, and $\Theta := \Sigma^{-1}$ be, if it exists, the precision matrix. We draw the edges so that the variables X_i, X_j are conditionally independent given the other variables if and only if the (i, j) -th element $\theta_{i,j}$ in Θ is 0:

$$\{i, j\} \notin E \iff \theta_{i,j} = 0 \iff X_i \perp\!\!\!\perp X_j | X_{V \setminus \{i,j\}},$$

where each edge is expressed as a set of two elements in $\{1, \dots, p\}$. In this sense, constructing a Gaussian graphical model is equivalent to estimating a precision matrix.

Suppose that we estimate the undirected graph from data consisting of n tuples of p variables and that dimension p is much higher than sample size n . For example, if we have expression data of $p = 20,000$ genes for $n = 100$ case/control patients, how can we construct a gene regulatory network

structure from the data? However, it is almost impossible to estimate the locations of the nonzero elements in Θ by obtaining the inverse of the estimate $S \in \mathbb{R}^{p \times p}$ of the covariance matrix Θ . In fact, if $p > n$, then no inverse S^{-1} exists because the rank of $S \in \mathbb{R}^{p \times p}$ is, at most, n .

To address the situation, two directions are suggested:

1. Sequentially find the variables on which each variable depends via regression so that the quasi-likelihood is maximized [Meinshausen et al., 2006]
2. Find the locations in Θ , the values of which are zeros, so that the ℓ_1 regularized log-likelihood is maximized [Yuan and Lin, 2007, Friedman et al., 2008, Banerjee et al., 2008, Rothman et al., 2008]

We follow the second approach because we assume Gaussian variables, also known as graphical lasso (GL). The ℓ_1 regularized log-likelihood is defined by

$$\max_{\Theta} \log \det \Theta - \text{trace} S \Theta - \lambda \|\Theta\|_1 \tag{1}$$

where tuning parameter λ controls the amount of sparsity, and $\|\Theta\|_1$ denotes the sum of the absolute value of the off-diagonal elements in Θ . Several optimization techniques [Banerjee et al., 2006, Mazumder and Hastie, 2012, Guillot et al., 2012, d’Aspremont et al., 2008, Friedman et al., 2008, Hsieh et al., 2014] have been studied for the optimization problem of (1).

In particular, we consider a generalized version of the abovementioned GL. For example, suppose that the gene regulatory networks of thirty case and seventy control patients are different. One might construct a gene regulatory network separately for each of the two categories. However, estimating each on its own does not provide an advantage if a common structure is shared. Instead, we use one hundred samples to construct two networks simultaneously. Intuitively speaking, using both types of data improves the reliability of the estimation by increasing the sample size for the genes that show similar values between case and control patients, while using only one type of data leads to a more accurate estimate for genes that show significantly different values. Danaher et al. [2014] proposed a joint graphical lasso (JGL) model by including an additional convex penalty (grouped lasso penalties) to the graphical lasso objective function for K classes. For example, K is two for the case/control in the example. Although there are several approaches to the problem, such as Honorio and Samaras [2010], Guo et al. [2011], Zhang and Wang [2012], Hara and Washio [2013], the JGL is considered the most promising.

The main topic of this paper is to improve efficiency in terms of solving the JGL problem. For the GL, a relatively efficient solving procedures exists. If we differentiate the ℓ_1 regularized log-likelihood by Θ , then we have an equation to solve [Friedman et al., 2008]. Moreover, several improvements have been considered for the GL, such as proximal Newton [Hsieh et al., 2014] and proximal gradient [Guillot et al., 2012] procedures. However, for the JGL, even if we derive such an equation, we have no efficient way to handle it.

Instead, the alternating direction method of multipliers (ADMM) [Glowinski and Marroco, 1975], which is a procedure for solving convex optimization problems for general purposes, has been the

Table 1: Efficient JGL Procedures

GL/JGL	Original	Proximal Newton	Proximal Gradient
GL	Friedman et al. [2008]	QUIC [Hsieh et al., 2014]	Guo et al. [2011]
JGL	Danaher et al. [2014]	Yang et al. [2015] (for fused penalty)	Current Paper

main approach taken [Danaher et al., 2014, Tang et al., 2015, Hallac et al., 2017, Gibberd and Nelson, 2017]. However, ADMM does not scale well concerning feature dimension p and number of classes K . It usually takes time for convergence to obtain high accuracy [Boyd et al., 2011].

For the efficient procedures of the JGL problem, Yang et al. [2015] proposed a method based on the proximal Newton procedure only when the penalty term is expressed by fused lasso (FMGL). The existing method requires expensive computations for the Hessian matrix and Newton directions, which means that it would be expensive for high-dimensional problems.

In this paper, we propose efficient proximal-gradient-based algorithms to solve the JGL problem by extending the procedure in Guillot et al. [2012] and modifying the step-size selection strategy proposed in Tran-Dinh et al. [2015]. Moreover, we provide the theoretical analysis of both methods for the JGL problem.

We show that the proposed methods are faster than ADMM and FMGL for any class K and large-scale p . Moreover, in our proximal gradient method for the JGL problem, the proximal operator in each iteration is quite simple, which eases the implementation process and requires very little computation and memory at each step. Simulation experiments are used to justify our proposed methods over the existing ones.

Our main contributions are as follows:

- We propose efficient algorithms based on the proximal gradient method to solve the JGL problem. The algorithms are first-order and quite simple, and the subproblems can be solved efficiently with a closed-form solution. The numerical results indicate that the methods can achieve high accuracy and precision, and the computational time is competitive with that of state-of-art algorithms.
- We provide the boundedness for the solution of the JGL problem and the iterations in algorithms. Then, the domain for the precision matrix in each iteration in our algorithms is constrained, guaranteeing the iterations inside the compact domain.

Table 1 summarizes the relationship between the proposed and existing methods.

The remaining parts of this paper are as follows. In Section 2, we first provide the background of our proposed method and introduce the joint graphical lasso problem. In Section 3, we illustrate the detailed content of the proposed algorithms and provide some theoretical analysis. In Section 4, we report some numerical results of the proposed approaches, including comparisons with efficient methods and performance evaluations. Finally, we draw some conclusions in Section 5.

2 Preliminaries

This section first reviews the graphical lasso (GL) problem and the G-ISTA algorithm [Guillot et al., 2012] to solve the GL problem. Then, we introduce the step-size selection strategy that we employed and the details of the joint graphical lasso problem.

2.1 Graphical lasso

Let $\mathbf{x}_1, \dots, \mathbf{x}_n \in \mathbb{R}^p$ be $n \geq 1$ observations of dimension $p \geq 1$ that follow the Gaussian distribution with mean $\boldsymbol{\mu} \in \mathbb{R}^p$ and covariance matrix $\boldsymbol{\Sigma} \in \mathbb{R}^{p \times p}$, where without loss of generality, we assume $\boldsymbol{\mu} = \mathbf{0}$. Let $\boldsymbol{\Theta} = \boldsymbol{\Sigma}^{-1}$, and the empirical covariance matrix $\mathbf{S} := \frac{1}{n} \sum_{i=1}^n \mathbf{x}_i^T \mathbf{x}_i$. Given penalty parameter $\lambda > 0$, the graphical lasso (GL) is the procedure to find the positive definite $\boldsymbol{\Theta} \in \mathbb{R}^{p \times p}$:

$$\underset{\boldsymbol{\Theta}}{\text{minimize}} -\log \det \boldsymbol{\Theta} + \text{trace}(\mathbf{S}\boldsymbol{\Theta}) + \lambda \|\boldsymbol{\Theta}\|_1, \quad (2)$$

where $\|\boldsymbol{\Theta}\|_1 = \sum_{j \neq k} |\theta_{j,k}|$. If we regard $V := \{1, \dots, p\}$ as a vertex set, then we can construct an undirected graph with edge set $\{\{j, k\} | \theta_{j,k} \neq 0\}$, where set $\{j, k\}$ denotes an undirected edge that connects the nodes $j, k \in V$.

If we take the subgradient of (2), then we find that the optimal solution $\boldsymbol{\Theta}_*$ satisfies the optimality condition:

$$\boldsymbol{\Theta}_*^{-1} - \mathbf{S} - \lambda \boldsymbol{\Phi} = \mathbf{0}, \quad (3)$$

where $\boldsymbol{\Phi} = (\Phi_{j,k})$ is

$$\Phi_{j,k} = \begin{cases} 1, & \theta_{j,k} > 0 \\ [-1, 1], & \theta_{j,k} = 0 \\ -1, & \theta_{j,k} < 0 \end{cases}.$$

2.2 ISTA for graphical lasso

In this section, we introduce the procedure for solving the GL problem (2) by the iterative shrinkage-thresholding algorithm (ISTA) proposed by Guillot et al. [2012], which is a proximal gradient method usually employed in dealing with nondifferentiable optimization problems.

Specifically, the general ISTA solves the following composite optimization problems:

$$\min_{\mathbf{x}} F(\mathbf{x}) := f(\mathbf{x}) + g(\mathbf{x}) \quad (4)$$

where f and g are convex functions, with f continuously differentiable and g possibly nonsmooth.

For the GL problem (2), denote $f, g : \mathbb{R}^{p \times p} \rightarrow \mathbb{R}$ as

$$f(\boldsymbol{\Theta}) := -\log \det \boldsymbol{\Theta} + \text{trace}(\mathbf{S}\boldsymbol{\Theta}),$$

and

$$g(\boldsymbol{\Theta}) := \lambda \|\boldsymbol{\Theta}\|_1.$$

If we define the quadratic approximation $Q_\eta : \mathbb{R}^{p \times p} \times \mathbb{R}^{p \times p} \rightarrow \mathbb{R}$ w.r.t. $f(\Theta)$:

$$Q_\eta(\Theta', \Theta) := f(\Theta) + \langle \Theta' - \Theta, \nabla f(\Theta) \rangle + \frac{1}{2\eta} \|\Theta' - \Theta\|_F^2, \quad (5)$$

then we can describe the ISTA as a procedure that iterates

$$\Theta_{t+1} = \arg \min_{\Theta} \{Q_{\eta_t}(\Theta, \Theta_t) + g(\Theta)\} \quad (6)$$

$$= \text{prox}_{\eta_t g}(\Theta_t - \eta_t \nabla f(\Theta_t)) \quad (7)$$

given initial value Θ_0 , where the value of step size η_t may change at each iteration $t = 1, 2, \dots$, and use the notation of the proximity operator:

$$\text{prox}_h(z) := \operatorname{argmin}_{\theta} \left\{ \frac{1}{2} \|z - \theta\|_2^2 + h(\theta) \right\}.$$

Note that the proximal operator of function $g = \lambda \|\Theta\|_1$ is the soft-thresholding operator: the absolute value $|\theta_{i,j}|$ of each off-diagonal element $\theta_{i,j}$ with $i \neq j$ becomes either $|\theta_{i,j}| - \lambda$ or zero (if $|\theta_{i,j}| < \lambda$). We use the following function in Sections 2.3 and 3:

$$\mathcal{S}_\lambda(\Theta) = \operatorname{sgn}(\theta_{i,j}) (|\theta_{i,j} - \lambda|)_+ \quad (8)$$

where $(x)_+ := \max(x, 0)$.

Definition 1. A differentiable function $f : \mathbb{R}^n \rightarrow \mathbb{R}$ is said to have a Lipschitz-continuous gradient if there exists $L > 0$ (Lipschitz constant) such that

$$\|\nabla f(\mathbf{x}) - \nabla f(\mathbf{y})\| \leq L \|\mathbf{x} - \mathbf{y}\|, \forall \mathbf{x}, \mathbf{y} \in \mathbb{R}^n \quad (9)$$

It is known that if we choose $\eta_t = 1/L$ for each step in the ISTA that minimizes $F(\cdot)$, then the convergence rate is, at most,

$$F(\Theta_t) - F(\Theta^*) = O(1/t) \quad (10)$$

[Beck and Teboulle, 2009]. However, for the GL problem (2), we know neither the exact value of the Lipschitz constant L nor any nontrivial upper bound. Guillot et al. [2012] implement a backtracking line search option in step 1 of Algorithm 1 below to handle this issue.

The backtracking line search means that we compute the η_t value for each time $t = 1, 2, \dots$ by repeatedly multiplying η_t by $0 < c < 1$ until $\Theta \succ 0$ (Θ is positive definite) and

$$f(\Theta_{t+1}) \leq Q_{\eta_t}(\Theta_{t+1}, \Theta_t) \quad (11)$$

for the Θ_{t+1} in (6), which means that $f(\Theta_t)$ is nonincreasing:

$$f(\Theta_{t+1}) \leq Q_{\eta_t}(\Theta_{t+1}, \Theta_t) \leq Q_{\eta_t}(\Theta_t, \Theta_t) = f(\Theta_t).$$

Additionally, (11) is a sufficient condition for (10), which was derived in Beck and Teboulle [2009] (see the relation between Lemma 2.3 and Theorem 3.1).

Moreover, the smaller η_t is, the more likely it satisfies condition (11). Θ_{t+1} is continuous w.r.t. η_t when Θ_t is fixed, which means that Θ_{t+1} trivially satisfies the condition for $\eta_t = 0$.

The whole procedure is given in the following algorithm, and we continue describing the third and fourth steps.

Algorithm 1 G-ISTA for problem (2)

Input: S, tolerance $\epsilon > 0$, backtracking constant $0 < c < 1$, initial value η_0, Θ_0 .

While $\Delta > \epsilon$ **do**

1: backtracking line search:

While

$$\Theta_{t+1} \succ 0 \quad \text{and} \quad f(\Theta_{t+1}) \leq Q_{\eta_t}(\Theta_{t+1}, \Theta_t) \quad (12)$$

 do not hold for $\Theta_{t+1} := \mathcal{S}_{\eta_t g}(\Theta_t - \eta_t \nabla f(\Theta_t))$ multiply η_t by c .

2: Update iterate: $\Theta_{t+1} \leftarrow \mathcal{S}_{\eta_t g}(\Theta_t - \eta_t \nabla f(\Theta_t))$

3: Set next initial step η_{t+1} by the Barzilai-Borwein gradient.

4: Compute duality gap: Δ

Output: ϵ -optimal solution to problem (1), $\Theta^* = \Theta_{t+1}$

The following properties provide a theoretical foundation that guarantees efficient convergence and suggest an efficient strategy for step size in the backtracking procedure and step 3.

Lemma 1. (Guillot et al. [2012], lemma 3) *Let $\{\Theta_t\}_{t=0,1,\dots}$ be the sequence generated by Algorithm 1, and Θ_* be the optimal solution of the problem (2); moreover, let*

$$a := \min\{\lambda_{\min}(\Theta_*), \lambda_{\min}(\Theta_t)\}$$

and

$$b := \max\{\lambda_{\max}(\Theta_*), \lambda_{\max}(\Theta_t)\},$$

where $\lambda_{\max}(\Theta_*)$ and $\lambda_{\min}(\Theta_*)$ are the maximum and minimum among the p eigenvalues of Θ_* , and $\lambda_{\max}(\Theta_t)$ and $\lambda_{\min}(\Theta_t)$ are the maximum and minimum among all the eigenvalues of Θ_t , $t = 1, 2, \dots$, respectively. Then, we have

$$\|\Theta_{t+1} - \Theta^*\|_F \leq \gamma \|\Theta_t - \Theta^*\|_F$$

with the convergence rate

$$\gamma := \max\left\{\left|1 - \frac{\eta_t}{b^2}\right|, \left|1 - \frac{\eta_t}{a^2}\right|\right\} .$$

Lemma 1 implies that to obtain $\gamma < 1$, we require

$$0 < \eta_t < a^2 \quad (13)$$

If the step size is in the range of (13), then the sequence $\{\Theta_t\}_{t=0,1,\dots}$ is bounded as follows:

Lemma 2. (Hsieh et al. [2014], Lemma2, Guillot et al. [2012], Theorem 2) *If the step size is in the range of (13), then all the iterations $\{\Theta_t\}_{t=0,1,\dots}$, belong to level set U defined as follows:*

$$U = \{\Theta_t | F(\Theta_t) \leq F(\Theta_0)\}$$

and we have

$$m \leq \|\Theta_t\| \leq M$$

for the constant $m := e^{-F(\Theta_0)}M^{-(p-1)}$, $M := \|\Theta^*\|_2 + \|\Theta_0 - \Theta^*\|_F$.

For each iteration of Algorithm 1, the initial step of η_t is needed. Guillot et al. [2012] considered step size $\eta := \lambda_{\min}(\Theta_t)^2$ using lemma 1 at first. However, it is quite conservative in practice. Hence, they used the Barzilai-Borwein method [Barzilai and Borwein, 1988] for implementation and regarded the step size η as safe. When the backtracking iterations in Step 1 exceed the given maximum number to satisfy condition (12), we can use the safe step for the subsequent calculations.

For Step 4, they considered the duality gap as a stopping criterion. The duality gap is defined as the difference between the primal and dual problems, which implies optimality when close to zero. To illustrate the duality gap in Step 4, we first introduce the dual problem of the GL problem (2).

$$\begin{aligned} \min_{\mathbf{U} \in \mathbb{R}^{p \times p}} \quad & -\log\det(\mathbf{S} + \mathbf{U}) - p \\ \text{subject to} \quad & \|\mathbf{U}\|_\infty \leq \lambda \end{aligned}$$

where \mathbf{U} are the dual variables, and the primal and dual variables are connected by $\Theta = (\mathbf{S} + \mathbf{U})^{-1}$. Hence, the duality gap of the GL problem in Step 4 is

$$\Delta := -\log\det(\mathbf{S} + \mathbf{U}_{t+1}) - p - \log\det\Theta_{t+1} + \langle \mathbf{S}, \Theta_{t+1} \rangle + \lambda \|\Theta_{t+1}\|_1$$

2.3 Composite self-concordant minimization

Tran-Dinh et al. [2015] considered a composite version of self-concordant minimization, which was initially proposed by Nesterov and Nemirovskii [1994]. Tran-Dinh et al. [2015] proposed a way to efficiently calculate the step size for the proximal gradient method for the GL problem. In particular, they proved that

$$f(\Theta) := -\log \det \Theta + \text{trace}(\mathbf{S}\Theta)$$

in (2) is self-concordant, and considers the minimization

$$F^* := \min_x \{F(x) := f(x) + g(x)\}$$

when f is convex, and self-concordant and when g is convex and nonsmooth. As for Algorithm 1, without using the backtracking line search, we can compute direction d_t :

$$\mathbf{d}_t := \mathcal{S}_{L_t^{-1}g}(\Theta_t - \eta_t \nabla f(\Theta_t)) - \Theta_t,$$

where \mathcal{S}_a with $a > 0$ defined by (8). Then, the step size can be determined by direction d_t . Let $L_t := \eta_t^{-1}$, $\beta_t := L_t \|\mathbf{d}_t\|_F^2$, $\lambda_t := \|\Theta_t^{-1} \mathbf{d}_t\|_F$, and the step size is

$$\alpha_t := \frac{\beta_t}{\lambda_t(\lambda_t + \beta_t)},$$

after that update $\Theta_{t+1} := \Theta_t + \alpha_t \mathbf{d}_t$ in the iterations.

In addition, Tran-Dinh et al. [2015] claimed that this strategy ensures a descent direction in the proximal gradient scheme and guarantees convergence.

2.4 Joint Graphical Lasso

Let $n \geq 1, p \geq 1, K \geq 2$, and $(\mathbf{x}_1, y_1), \dots, (\mathbf{x}_n, y_n) \in \mathbb{R}^p \times \{1, \dots, K\}$, where each x_i is a row vector. Let n_k be the number of occurrences in y_1, \dots, y_n such that $y_i = k$, so that $\sum_{k=1}^K n_k = n$.

For each $k = 1, \dots, K$, we define the empirical covariance matrix $\mathbf{S}^{(k)} \in \mathbb{R}^{p \times p}$ of the data \mathbf{x}_i as follows:

$$\mathbf{S}^{(k)} := \frac{1}{n_k} \sum_{i: y_i=k} \mathbf{x}_i^T \mathbf{x}_i$$

Given the penalty parameters $\lambda_1 > 0$ and $\lambda_2 > 0$, the joint graphical lasso (JGL) is the procedure to find the positive definite matrix $\Theta^{(k)} \in \mathbb{R}^{p \times p}$ for $k = 1, \dots, K$, such that

$$\min_{\Theta} - \sum_{k=1}^K n_k \{\log \det \Theta^{(k)} - \text{trace}(\mathbf{S}^{(k)} \Theta^{(k)})\} + \lambda_1 \sum_{k=1}^K \sum_{i \neq j} |\theta_{i,j}^{(k)}| + P(\Theta), \quad (14)$$

where $P(\Theta)$ penalizes $\Theta := [\Theta_1, \dots, \Theta_K]^T$, and the choices are diverse. For example, Danaher et al. [2014] suggested the fused and group lasso penalties:

$$P_F(\Theta) := \lambda_2 \sum_{k \neq l} \sum_{i,j} |\theta_{k,i,j} - \theta_{l,i,j}|$$

and

$$P_G(\Theta) := \lambda_2 \sum_{i \neq j} \left\{ \sum_{k=1}^K \theta_{k,i,j}^2 \right\}^{1/2},$$

where $\theta_{k,i,j}$ is the (i, j) -th element of $\Theta^{(k)} \in \mathbb{R}^{p \times p}$ for $k = 1, \dots, K$.

Lemma 3. (Yang et al. [2015]) *Under the assumption that $\text{diag}(\mathbf{S}^{(k)}) > 0, k = 1, \dots, K$, problem (14) has a unique optimal solution.*

Lemma 3 shows the uniqueness of problem (14). Unfortunately, there is no equation like (3) for the JGL to find the optimum Θ_* . Danaher et al. [2014] considered the ADMM to solve the JGL problem. However, ADMM is quite time-consuming for large-scale problems.

3 Proposed Method

In this section, we propose two efficient algorithms for solving the JGL problem. One is an extended ISTA based on the G-ISTA, and we modify the other by the step-size selection strategy illustrated in Section 2.3.

3.1 ISTA for JGL problem

To neatly describe the JGL problem, we define $f, g : \mathbb{R}^{K \times p \times p} \rightarrow \mathbb{R}$ by

$$f(\Theta) := - \sum_{k=1}^K n_k \{\log \det \Theta^{(k)} - \text{trace}(\mathbf{S}^{(k)} \Theta^{(k)})\} \quad (15)$$

$$g(\Theta) := \lambda_1 \sum_{k=1}^K \|\Theta^{(k)}\|_1 + P(\Theta) \quad (16)$$

Then, the problem (14) becomes the following:

$$\min_{\Theta} F(\Theta) := f(\Theta) + g(\Theta)$$

$f(\Theta)$ is convex and continuously differentiable, and $g(\Theta)$ is convex and nonsmooth. Therefore, the ISTA is available for solving the JGL problem (14).

The main differences between the G-ISTA and the proposed method are that the latter needs to consider K categories of graphical models simultaneously in the JGL problem (14). There are two combined penalties in $g(\Theta)$, which complicate the proximal operator in the ISTA procedure. Consequently, the operator for the proposed method is not a simple soft thresholding operator, as is that for the G-ISTA method.

If we define quadratic approximation $Q_{\eta_t} : \mathbb{R}^{K \times p \times p} \rightarrow \mathbb{R}$ of $f(\Theta)$:

$$\begin{aligned} Q_{\eta_t}(\Theta, \Theta_t) := & - \sum_{k=1}^K n_k \{ \log \det \Theta^{(k)} - \text{trace}(\mathbf{S}^{(k)} \Theta^{(k)}) \} \\ & + \sum_{k=1}^K \langle \Theta^{(k)} - \Theta_t^{(k)}, \nabla f(\Theta_t^{(k)}) \rangle + \frac{1}{2\eta_t} \sum_{k=1}^K \|\Theta^{(k)} - \Theta_t^{(k)}\|_F^2, \end{aligned}$$

then the update iteration becomes the following:

$$\Theta_{t+1} = \underset{\Theta}{\text{argmin}} \{ Q_{\eta_t}(\Theta, \Theta_t) + g(\Theta) \} = \text{prox}_{\eta_t g}(\Theta_t - \eta_t \nabla f(\Theta_t))$$

Nevertheless, the Lipschitz gradient constant of $f(\Theta)$ is unknown over the whole domain in the JGL problem. Therefore, our approach also needs a backtracking line search to calculate step size η_t . We show the details in Algorithm 2.

Algorithm 2 ISTA for problem (14)

Input: \mathbf{S} , tolerance $\epsilon > 0$, backtracking constant $0 < c < 1$, initial value η_0, Θ_0 .

For $t = 0, 1, \dots$, (until convergence) **do**

1: backtracking line search: While

$$f(\Theta_{t+1}) \leq Q_{\eta_t}(\Theta_{t+1}, \Theta_t) \text{ and } \Theta_{t+1}^{(k)} \succ 0 \text{ for } k = 1, \dots, K \quad (17)$$

do not hold for $\Theta_{t+1} := \text{prox}_{\eta_t g}(\Theta_t - \eta_t \nabla f(\Theta_t))$ multiply η_t by c .

2: Update iterate: $\Theta_{t+1} \leftarrow \text{prox}_{\eta_t g}(\Theta_t - \eta_t \nabla f(\Theta_t))$

3: Set next initial step η_{t+1}

Output: ϵ -optimal solution to problem (1), $\Theta^* = \Theta_{t+1}$

After obtaining step size η_t , we discuss the detailed calculation of the proximal operator for fused lasso and group lasso penalties. In the following, we will see that the subproblems of the proximal operator for the two types of penalties are equivalent to the fused lasso and group lasso problems, respectively, and can be solved easily by any associated efficient procedure.

A. Fused lasso penalty P_F

By the definition of the proximal operator in the update step, we have

$$\Theta_{t+1} = \arg \min_{\Theta} \left\{ \frac{1}{2} \|\Theta - \Theta_t + \eta_t \nabla f(\Theta_t)\|^2 + \eta_t \cdot \lambda_1 \sum_{k=1}^K \sum_{i \neq j} |\theta_{k,i,j}| + \eta_t \cdot \lambda_2 \sum_{k \neq l} \sum_{i,j} |\theta_{k,i,j} - \theta_{l,i,j}| \right\} \quad (18)$$

Problem (18) is separable with respect to the elements $\theta_{k,i,j}$ in $\Theta^{(k)} \in \mathbb{R}^{p \times p}$; hence, the proximal operator can be computed in componentwise operations:

Let $A = \Theta_t - \eta_t \nabla f(\Theta_t)$; then, problem (18) reduces to the following subproblem for $i = 1, \dots, p$, $j = 1, \dots, p$:

$$\operatorname{argmin}_{\theta_{1,i,j}, \dots, \theta_{K,i,j}} \left\{ \frac{1}{2} \sum_{k=1}^K (\theta_{k,i,j} - a_{k,i,j})^2 + \eta_t \cdot \lambda_1 \cdot 1_{i \neq j} \sum_{k=1}^K |\theta_{k,i,j}| + \eta_t \cdot \lambda_2 \sum_{k \neq l} |\theta_{k,i,j} - \theta_{l,i,j}| \right\} \quad (19)$$

where $1_{i \neq j}$ is an indicator function, the value of which is 1 only when $i \neq j$. Then, this is known as the fused lasso signal approximator (FLSA) [Friedman et al., 2007]. Several rather efficient algorithms can be used to solve this problem [Hoeffling, 2010, Tibshirani et al., 2011, Johnson, 2013].

In particular, for illustration, let $\alpha_1 := \eta_t \cdot \lambda_1 \cdot 1_{i \neq j}$ and $\alpha_2 := \eta_t \cdot \lambda_2$. When $i = j$, $\alpha_1 = 0, \alpha_2 > 0$, subproblem (19) solves the FLSA problem with K -dimensional variable $\theta_{k,i,j}$.

When $i \neq j$, $\alpha_1 > 0$, the solution to (19) can be obtained through soft thresholding based on the solution when $\alpha_1 = 0$ by the following lemma.

Lemma 4. (Friedman et al. [2007]) *Assume that the solutions to $\alpha_1 = 0$ and α_2 are known and denoted by $\theta_k(0, \alpha_2)$. Then, the solution for $\alpha_1 > 0$ in the fused lasso problem is*

$$\theta_k(\alpha_1, \alpha_2) = \mathcal{S}_{\alpha_1}(\theta_k(0, \alpha_2)) \quad \text{for } k = 1 \dots, K$$

B. Group lasso penalty P_G

By definition, the update of Θ_{t+1} for group lasso penalty $P_G(\Theta)$ is:

$$\Theta_{t+1} = \arg \min_{\Theta} \left\{ \frac{1}{2} \|\Theta - \Theta_t + \eta_t \nabla f(\Theta_t)\|^2 + \eta_t \cdot \lambda_1 \sum_{k=1}^K \sum_{i \neq j} |\theta_{k,i,j}| + \eta_t \cdot \lambda_2 \sum_{i \neq j} \left(\sum_{k=1}^K \theta_{k,i,j}^2 \right)^{\frac{1}{2}} \right\}$$

Similarly, let $A = \Theta_t - \eta_t \nabla f(\Theta_t)$; then, the problem becomes

$$\operatorname{argmin}_{\theta_{1,i,j}, \dots, \theta_{K,i,j}} \left\{ \frac{1}{2} \sum_{k=1}^K (\theta_{k,i,j} - a_{k,i,j})^2 + \eta_t \cdot \lambda_1 \cdot 1_{i \neq j} \sum_{k=1}^K |\theta_{k,i,j}| + \eta_t \cdot \lambda_2 \cdot 1_{i \neq j} \left(\sum_{k=1}^K \theta_{k,i,j}^2 \right)^{\frac{1}{2}} \right\}.$$

Obviously, when $i = j$, $\theta_{k,i,j} = a_{k,i,j}$. For $i \neq j$, it is a group lasso problem [Yuan and Lin, 2006, Friedman et al., 2010], and we can simply solve it by the following Friedman et al. [2010]:

$$\theta_{k,i,j} = \mathcal{S}_{\eta_t \cdot \lambda_1}(a_{k,i,j}) \left(1 - \frac{\eta_t \cdot \lambda_2}{\sqrt{\sum_{k=1}^K \mathcal{S}_{\eta_t \cdot \lambda_1}(a_{k,i,j})^2}} \right)_+.$$

3.1.1 Theoretical analysis

In the following claim, we extend the theoretical analysis in Section 2 to the JGL problem and show that the optimal solution Θ_* in the JGL problem can be bounded.

As we can see in Lemma 2, the bounds of Θ_t in Algorithm 1 are related to the bounds of Θ_* , which were already proven by Banerjee et al. [2008] and Lu [2009]. For multiple Gaussian graphical models, Honorio and Samaras [2010] and Hara and Washio [2013] provided the bounds for the optimal solution $\Theta_*^{(k)}$. However, though their target models were similar, they were different from those of the JGL model. To the best of our knowledge, no related research has provided the bounds of the optimal solution $\Theta_*^{(k)}$ for the JGL problem.

In the following, we provide the lower and upper bounds for $\Theta_*^{(k)}$, which are applied to both fused and group lasso-type penalties.

Proposition 1. *The optimal solution Θ^* of the problem (14) satisfies*

$$\frac{n_k}{p\lambda_c + n_k\|S^{(k)}\|_2} \leq \|\Theta_*^{(k)}\|_2 \leq \frac{Np}{\lambda_1} + \sum_{k=1}^K \sum_{i=1}^p (s_{ii}^{(k)})^{-1}$$

where $\lambda_c := \sqrt{K\lambda_1^2 + 2K\lambda_1\lambda_2 + \lambda_2^2}$.

We use the same G-ISTA strategy to handle the initial step size of η_t for each iteration in Algorithm 2. In the numerical experiment (section 4.2.3), the algorithm also shows a linear convergence rate.

3.2 Modified ISTA for JGL

In the previous discussion, we mentioned that $f(\Theta)$ in the JGL problem is not globally Lipschitz gradient continuous. The ISTA may not be efficient enough for the JGL case because it includes the backtracking line search procedure for this case, which needs to evaluate the objective function and is inefficient when the evaluation is expensive.

In this section, we modify Algorithm 2 to Algorithm 3 based on the strategy in Section 2.3, which takes advantage of the properties of the self-concordant function. The self-concordant function does not rely on the Lipschitz gradient assumption on the smooth part $f(\Theta)$ [Tran-Dinh et al., 2015], and we can eliminate the need for the backtracking line search.

Lemma 5. *(Boyd et al. [2004]) Self-concordance is preserved by scaling and addition: if f is a self-concordant function and a constant $a \leq 1$, then af is self-concordant. If f_1, f_2 are self-concordant, then $f_1 + f_2$ is self-concordant.*

By Lemma 5, the function (15) is a self-concordant function. In Algorithm 3, for the initial step size of L_t^{-1} in each iteration, we use the same strategy as that of Algorithm 2. Then, the mechanism in Tran-Dinh et al. [2015] is employed in Steps 3-5 of Algorithm 3.

Algorithm 3 Modified ISTA algorithm

Input: \mathbf{S} , tolerance $\epsilon > 0$, initial step size L_0^{-1} , initial iterate Θ_0 .

For $t = 0, 1, \dots$, (until convergence) **do**

1: Initialize L_t

2: Compute

$$\mathbf{d}_t := \text{prox}_{L_t^{-1}g}(\Theta_t - L_t^{-1}\nabla f(\Theta_t)) - \Theta_t \quad (20)$$

3: Compute $\beta_t := L_t \|\text{vec}(\mathbf{d}_t)\|_2^2$ and $\lambda_t := \sum_{k=1}^K n_k \|(\Theta_t^{(k)})^{-1} \mathbf{d}_t^{(k)}\|_2$.

4: Determine step size $\alpha_t := \frac{\beta_t}{\lambda_t(\lambda_t + \beta_t)}$

5: If $\alpha_t > 1$, then set $L_t := \frac{L_t}{2}$ and go back to Step 2

6: Update $\Theta_{t+1} := \Theta_t + \alpha_t \mathbf{d}_t$

Output: ϵ -optimal solution to problem (1), $\Theta^* = \Theta_{t+1}$

However, there is no backtracking procedure in this algorithm that guarantees the positive definiteness of Θ_t , as in (17) of Algorithm 2. Hence, in Algorithm 3, we need to illustrate how to ensure the positive definiteness of the Θ_{t+1} in the iterations.

Lemma 6. (Nemirovski [2004], Theorem 2.1.1) *Let f be a self-concordant function and let $x \in \text{dom} f$. Additionally, if*

$$W_r(\mathbf{x}) = \{\mathbf{y} | (\mathbf{y} - \mathbf{x}) \nabla^2 f(\mathbf{x}) (\mathbf{y} - \mathbf{x}) \leq 1\}$$

then $W_r(\mathbf{x}) \subset \text{dom} f$.

In Algorithm 3, because we know $\alpha_t := \frac{\beta_t}{\lambda_t(\lambda_t + \beta_t)}$ and $\alpha_t \leq 1$ by Step 3 and 5, therefore $\alpha_t^2 \lambda_t < 1$, i.e.:

$$\begin{aligned} \alpha_t^2 \lambda_t &= \alpha_t^2 \sum_{k=1}^K n_k \|(\Theta_t^{(k)})^{-1} \mathbf{d}_t^{(k)}\|_2 < 1 \\ (\Theta_{t+1} - \Theta_t) \nabla^2 f(\Theta_t) (\Theta_{t+1} - \Theta_t) &< 1 \end{aligned}$$

Hence, by Lemma 6, the Θ_{t+1} stays in the domain and keeps the positive definiteness.

By Lemma 12 in Tran-Dinh et al. [2015], it is known that the function value is always decreasing in Algorithm 3:

$$F(\Theta_{t+1}) \leq F(\Theta_t) \quad \text{for } t = 0, 1, \dots, \quad (21)$$

Then, based on condition (21), we provide the explicit bounds of $\{\Theta_t\}_{t=0,1,\dots}$, in Algorithm 3 for the JGL problem with the help of Lemma 2 and Proposition 1. For the proof, see Appendix.

Proposition 2. *Sequence $\{\Theta_t\}_{t=0,1,\dots}$, generated by Algorithm 3 can be bounded:*

$$m \leq \|\Theta_t\|_2 \leq M$$

where $M := \|\Theta_0\|_F + 2\|\Theta_*\|_F$, $m := e^{-\frac{C_1}{n_m}} M^{(1-Kp)}$, $n_m = \max_k n_k$, and constant $C_1 := F(\Theta_0)$.

4 Experiments

In this section, we evaluate the performance of the proposed method on both synthetic and real datasets, and we compare the following algorithms:

- ADMM: the general ADMM method proposed by Danaher et al. [2014]
- FMGL: the proximal Newton-type method proposed by Yang et al. [2015].
- ISTA: the proposed method in Algorithm 2.
- M-ISTA: the proposed method in Algorithm 3.

We perform all the tests in R Studio on a Macbook Air with 1.6 GHz Intel Core i5 and 8 GB memory. The wall times are recorded as the run times for the four algorithms.

4.1 Stopping criteria

In the experiments, we consider two stopping criteria for the algorithms.

1. Relative error:

$$\frac{\sum_{k=1}^K \|\Theta_{t+1}^{(k)} - \Theta_t^{(k)}\|_F}{\max\{\sum_{k=1}^K \|\Theta_t^{(k)}\|_F, 1\}} \leq \epsilon$$

2. Objective error:

$$\|F(\Theta_t) - F(\Theta_*)\|_F \leq \epsilon$$

We use the objective error for convergence rate analysis and the relative error for the time comparison. Because, in our proposed method, we do not obtain dual solutions, we do not employ the duality gap stopping criterion in Section 2.2.

4.1.1 Model selection

The JGL model is affected by regularized parameters λ_1 and λ_2 . For selecting the parameters, we use the D -fold cross-validation method. First, the dataset is randomly split into D segments of equal size, a single subset (test data), estimated by the other $D - 1$ subsets (training data) and change the subset for the test to repeat D times so that each subset is used.

Let $S_d^{(k)}$ be the sample covariance matrix of d -th ($d = 1, \dots, D$) segment for class $k = 1, \dots, K$. We estimate the inverse covariance matrix by the remaining $D - 1$ subsets $\hat{\Theta}_{\lambda, -d}^{(k)}$, and choose λ_1 and λ_2 that minimize the average predictive negative log-likelihood as follows:

$$CV(\lambda_1, \lambda_2) = \sum_{d=1}^D \sum_{k=1}^K \left\{ n_k \text{trace}(S_d^{(k)} \hat{\Theta}_{\lambda, -d}^{(k)}) - \log \det \hat{\Theta}_{\lambda, -d}^{(k)} \right\}.$$

4.2 Synthetic data

We follow the data generation mechanism described in Li and Gui [2006] with some modifications for the JGL model. We put the details in Appendix.

The performance of the proposed methods was assessed on synthetic data in terms of the number of iterations, the execution time, the squared error, and the receiver operating characteristic (ROC) curve.

4.2.1 Comparison experiments

We vary p, N, K and λ_1 to compare the execution time of our proposed methods with that of the existing methods. For a fair comparison in the experiments, we consider only the fused penalty in our proposed method because the FMGL algorithm applies only to the fused penalty. First, we compare the performance among different algorithms under various dimensions p , which are shown in Figure 1.

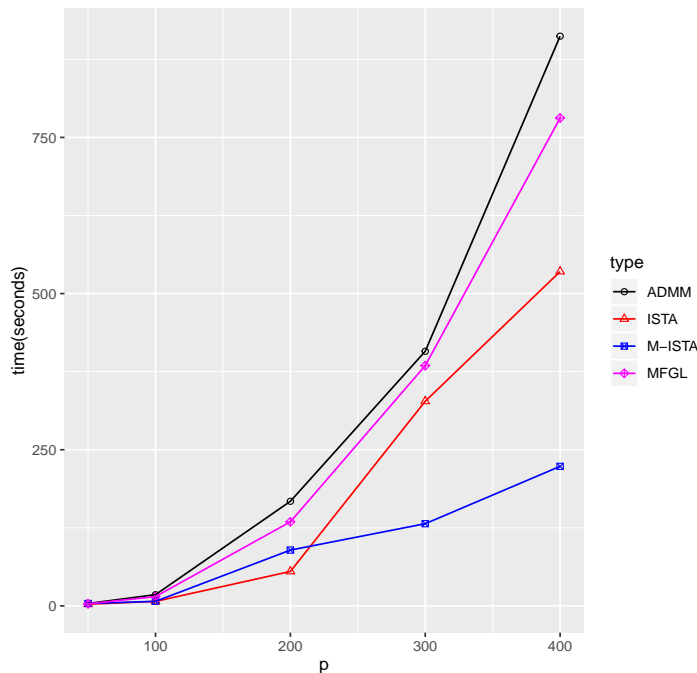


Figure 1: Plot of time comparison under different p . Setting $\lambda_1 = 0.1, \lambda_2 = 0.05, K = 2$ and $N = 200$.

Figure 1 shows that the execution time of the FMGL and ADMM increases rapidly as p increases. In particular, we observe that the M-ISTA significantly outperforms when p exceeds 200. The ISTA shows better performance than the three methods when p is less than 200, but it requires more time as p grows, compared to the M-ISTA. It is reasonable to consider that evaluating the objective function in the backtracking line search at every iteration increases the computational burden, especially when

p increases, which means that the M-ISTA is a good choice for these cases. Furthermore, the ISTA can be a good candidate when the evaluation is inexpensive.

Table 2: Computational time under different settings

Parameters setting					Computational time				
p	K	N	1	2	precision ϵ	ADMM	FMGL	ISTA	M-ISTA
20	2	50	0.1	0.05	0.00001	10.506 secs	1.158 secs	2.174 secs	1.742 secs
	5		1	0.5		1.123mins	10.556 secs	4.216 secs	2.874 secs
30	2	120	0.1	0.05	0.0001	36.592 secs	13.225 secs	12.675 secs	12.700 secs
	3		0.1	0.05		3.779 mins	2.424 mins	58.208 secs	1.481 mins
50	2	600	0.02	0.005	0.0001	6.427 secs	10.228 secs	7.213 secs	4.625 secs
			0.03			6.240 secs	8.925 secs	6.645 secs	4.023 secs
			0.04			7.025 secs	9.381 secs	6.144 secs	3.993 secs
200	2	400	0.09	0.05	0.0001	4.050 mins	1.874 mins	2.289 mins	35.038 secs
			0.1			4.569 mins	1.137 mins	1.340 mins	24.852 secs
			0.12			3.848 mins	1.881 mins	1.443 mins	18.367 secs

Table 2 summarizes the performance of the four algorithms under different parameter settings for achieving a given precision ϵ of the relative error. The results presented in Table 2 reveals that when we increase the number of classes K , all the algorithms spend more time than usual. Moreover, the execution time of ADMM becomes huge among them. When we vary the λ_1 , they become more efficient as the value larger. For most instances, the M-ISTA and ISTA outperform the existing ones, such as ADMM and FMGL. As for the exceptional cases ($p = 20, k = 2, N = 50, \lambda_1 = 0.1$ and $\lambda_2 = 0.05$), the M-ISTA is still comparable with the FMGL and faster than ADMM.

4.2.2 Algorithm Assessment

We assessed our proposed method by drawing a receiver operating characteristic (ROC) curve, which displays the number of true positive edges (i.e., TP edges) selected against the number of false edges (i.e., FP edges) selected. We say that an edge (i, j) in the k -th class is selected in estimate $\hat{\Theta}^{(k)}$ if element $\hat{\theta}_{ij}^{(k)} \neq 0$ and the edges are true positive edges selected if the precision matrix $\theta_{ij}^{(k)} \neq 0$ and false positive edges selected if the precision matrix $\theta_{ij}^{(k)} = 0$, where the two quantities are defined by

$$TP = \sum_{k=1}^K \sum_{i < j} 1(\theta_{ij}^{(k)} = 0) \cdot 1(\hat{\theta}_{ij}^{(k)} = 0) ,$$

$$FP = \sum_{k=1}^K \sum_{i < j} 1(\theta_{ij}^{(k)} \neq 0) \cdot 1(\hat{\theta}_{ij}^{(k)} = 0) ,$$

and $1(\cdot)$ is the indicator function.

To confirm the validity of the proposed method, we compare the ROC figures of the fused penalty and group penalty. We fix the parameters λ_2 for each curve and change the λ_1 value to obtain

various numbers of selected edges because the sparsity penalty parameter λ_1 can control the number of selected total edges.

First, we show the ROC curves for fused and group lasso penalties in Figure 2a and Figure 2b, respectively.

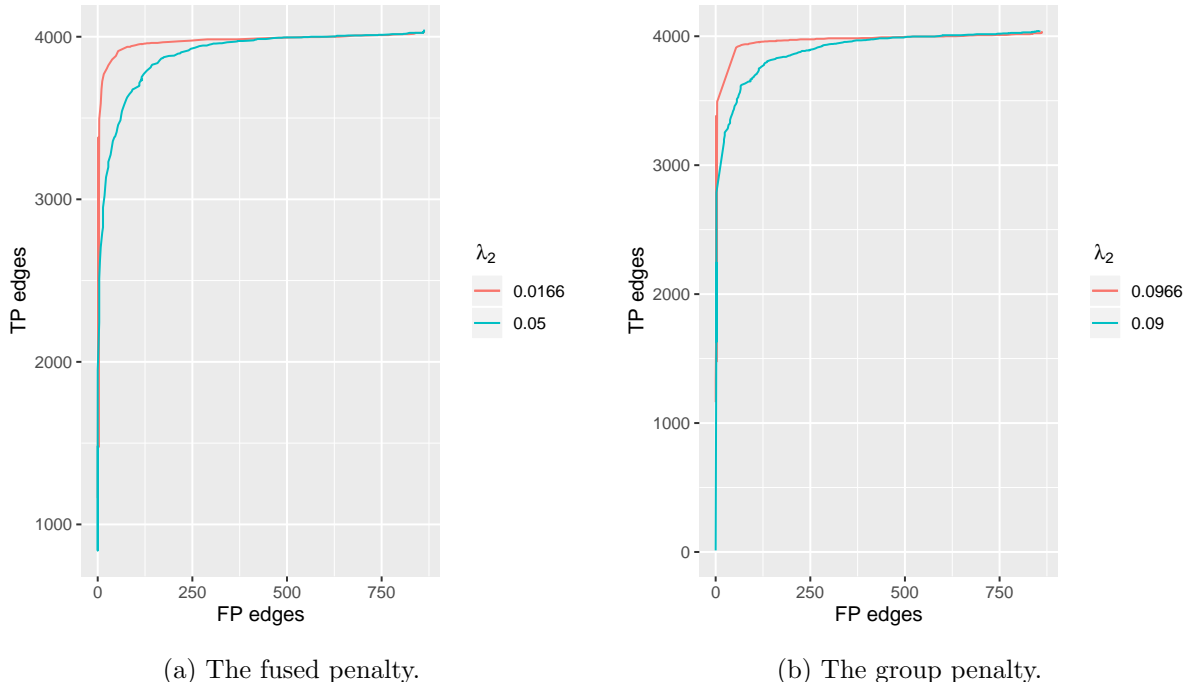


Figure 2: Plot of true positive edges vs. false positive edges selected. Setting $p=50$, $K=2$.

From the figures, we observe that both penalties show highly accurate predictions for the edge selections. The result of $\lambda_2 = 0.0166$ in the fused penalty case is better than that in $\lambda_2 = 0.05$. Additionally, the result of $\lambda_2 = 0.0966$ in the fused penalty case is better than that in $\lambda_2 = 0.09$, which means that if we select the tuning parameters properly, then we can obtain precise results while simultaneously meeting our different model demands.

Then, Figure 3a and Figure 3b display the mean squared errors (MSE) between the estimated values and true values.

$$MSE = \frac{2}{Kp(p-1)} \sum_{k=1}^K \sum_{i < j} (\hat{\theta}_{ij}^{(k)} - \theta_{ij}^{(k)})^2$$

where $\hat{\theta}_{ij}^{(k)}$ is the value estimated by the proposed method, and $\theta_{ij}^{(k)}$ is the true precision matrix value we use in the data generation.

The figures illustrate that when the total number of edges selected is increasing, the errors decrease and finally achieve relatively low values.

Overall, the proposed method shows competitive efficiency not only in computational time but also in accuracy.

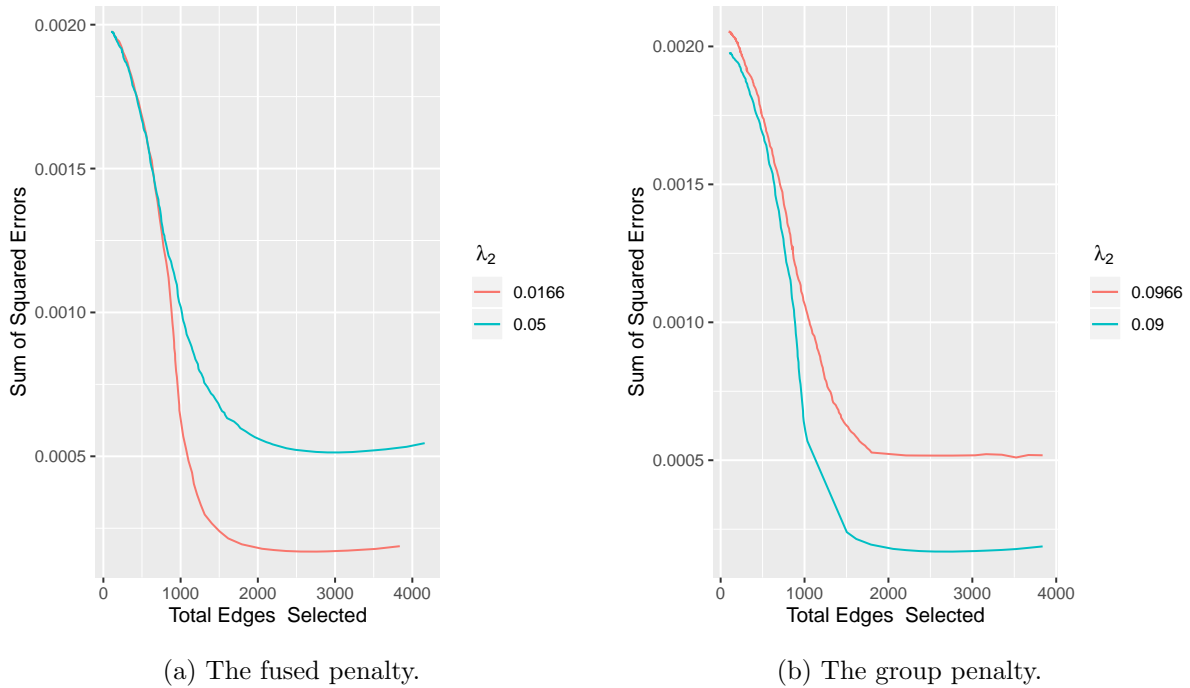


Figure 3: Plot of the mean squared errors vs. total edges selected. Setting $p=50$, $K=2$.

4.2.3 Convergence rate

This section shows the convergence rate of the ISTA for the JGL problem in practice, with $\lambda_1 = 0.1, 0.09$ and 0.08 . We recorded the number of iterations to achieve the different tolerance of $F(\Theta_t) - F(\Theta_*)$ and ran it on a synthetic dataset, with $p = 200, K = 2, \lambda_2 = 0.05$ and $N = 400$. The figure reveals that as λ_1 decreases, more iterations are needed to converge to the specified tolerance. Moreover, the figure shows the linear convergence rate of the proposed ISTA method.

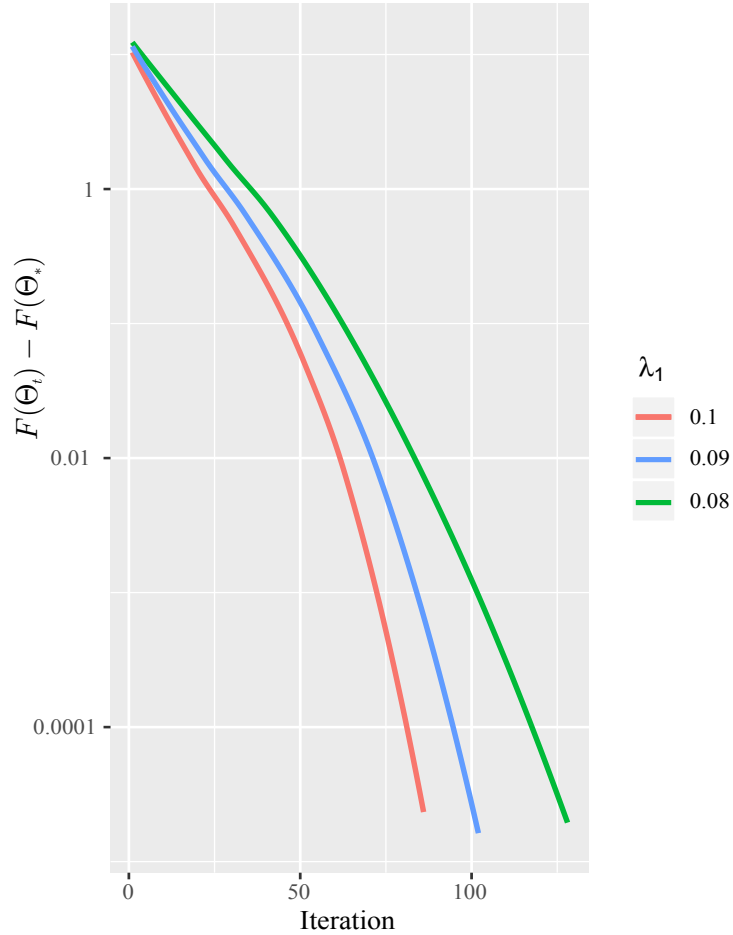


Figure 4: Plot of $\log(F(\Theta_t) - F(\Theta_*))$ vs. the number of iterations with different λ_1 values. Setting $p = 200, N = 400, K = 2$ and $\lambda_2 = 0.05$.

4.3 Real data

We use a breast cancer dataset for the experiment to show the common structure and jointly estimate common links across graphs. There are 250 samples and 1,000 types of genes in the dataset, with 192 control samples and 58 case samples. Additionally, we set $\lambda_1 = 0.3, \lambda_2 = 0.08$ for suitable visualization.

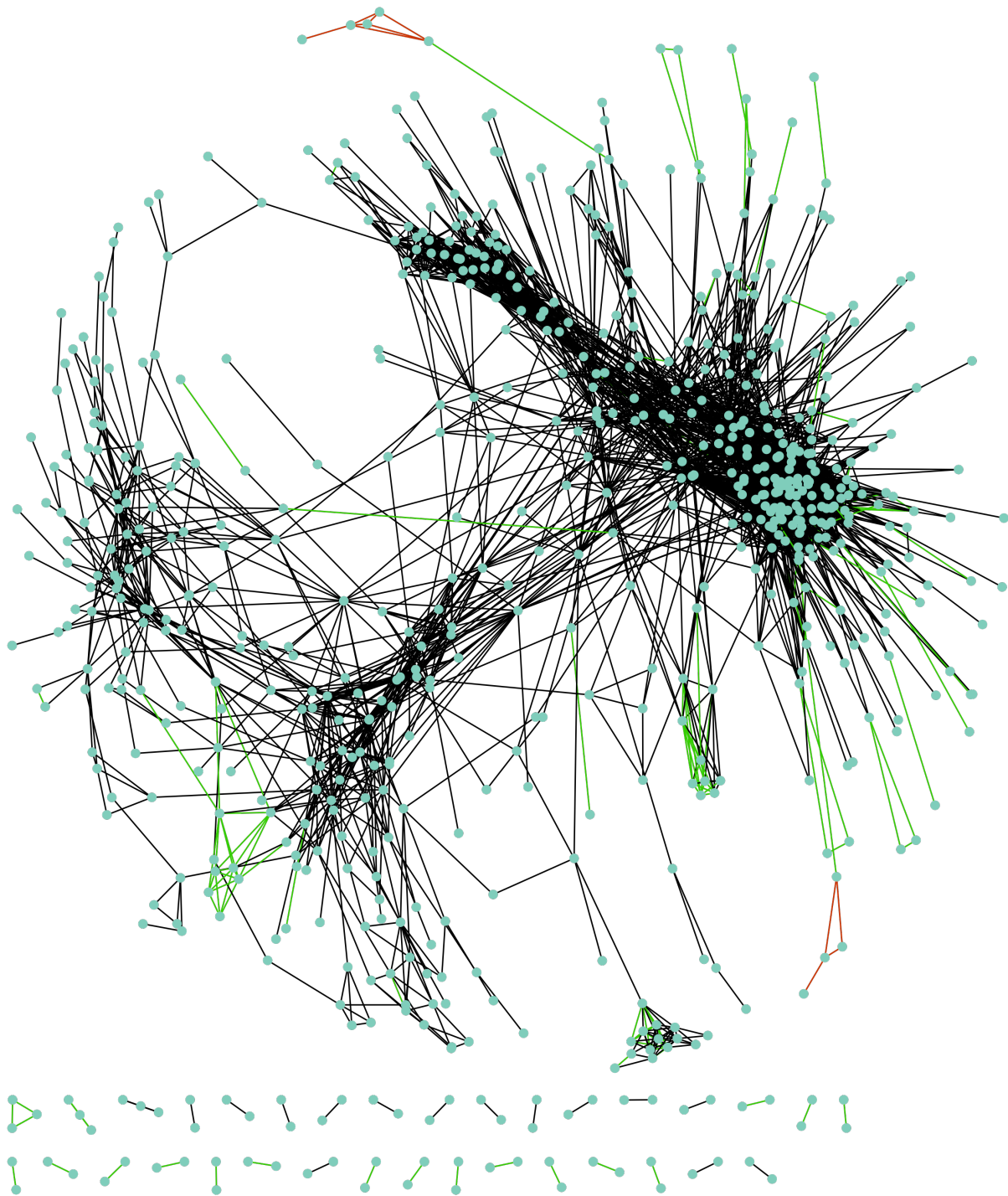


Figure 5: Graph of the gene expression of breast cancer

We use Cytoscape [Shannon et al., 2003] to visualize the results. Figure 5 shows the graph of the breast cancer gene expression identified by the JGL model with the proposed methods. As we can see in the figure, each node represents a gene, and the edges demonstrate the relationship between

genes.

We use different colors to show various structures. The green edges are a common structure between the two classes, the red edges are the specific structures for the control classes, and the black edges are for the case samples.

5 Conclusions

We propose two efficient proximal gradient descent procedures with and without the backtracking line search option for the joint graphical lasso. The first does not require extra variables, unlike ADMM, which needs manual tuning of the Lagrangian parameters and dual variables. Moreover, we reduce it to subproblems that can be solved both efficiently and precisely. The second does not require backtracking line search, which significantly reduces the computation time needed to evaluate objective functions.

From the theoretical perspective, we reach the linear convergence rate for the ISTA. Furthermore, we derive the lower and upper bounds of the solution to the JGL problem and the iterations in the algorithms, guaranteeing that the iterations stay in the constrained domain. Numerically, the methods are demonstrated on both simulated and real datasets to illustrate their robust and efficient performance over state-of-the-art algorithms.

For the further computational improvement, the most expensive step in the algorithms is to calculate the inversion of matrices required by the gradient of $f(\Theta)$. Both algorithms have a complexity of $O(Kp^3)$ per iteration. Moreover, we can solve the matrix inversion problem with more efficient algorithms with lower complexity. In addition, we can also use the faster computation procedure in Danaher et al. [2014] to decompose the optimization problem for the proposed methods and regard it as preprocessing. Overall, the proposed methods are highly efficient for the joint graphical lasso problem.

References

- Onureena Banerjee, Laurent El Ghaoui, Alexandre d’Aspremont, and Georges Natsoulis. Convex optimization techniques for fitting sparse gaussian graphical models. In *Proceedings of the 23rd international conference on Machine learning*, pages 89–96, 2006.
- Onureena Banerjee, Laurent El Ghaoui, and Alexandre d’Aspremont. Model selection through sparse maximum likelihood estimation for multivariate gaussian or binary data. *The Journal of Machine Learning Research*, 9:485–516, 2008.
- Jonathan Barzilai and Jonathan M Borwein. Two-point step size gradient methods. *IMA journal of numerical analysis*, 8(1):141–148, 1988.
- Amir Beck and Marc Teboulle. A fast iterative shrinkage-thresholding algorithm for linear inverse problems. *SIAM journal on imaging sciences*, 2(1):183–202, 2009.
- Stephen Boyd, Stephen P Boyd, and Lieven Vandenbergh. *Convex optimization*. Cambridge university press, 2004.
- Stephen Boyd, Neal Parikh, and Eric Chu. *Distributed optimization and statistical learning via the alternating direction method of multipliers*. Now Publishers Inc, 2011.
- Patrick Danaher, Pei Wang, and Daniela M Witten. The joint graphical lasso for inverse covariance estimation across multiple classes. *Journal of the Royal Statistical Society. Series B, Statistical methodology*, 76(2):373, 2014.
- Alexandre d’Aspremont, Onureena Banerjee, and Laurent El Ghaoui. First-order methods for sparse covariance selection. *SIAM Journal on Matrix Analysis and Applications*, 30(1):56–66, 2008.
- Jerome Friedman, Trevor Hastie, Holger Höfling, Robert Tibshirani, et al. Pathwise coordinate optimization. *Annals of applied statistics*, 1(2):302–332, 2007.
- Jerome Friedman, Trevor Hastie, and Robert Tibshirani. Sparse inverse covariance estimation with the graphical lasso. *Biostatistics*, 9(3):432–441, 2008.
- Jerome Friedman, Trevor Hastie, and Robert Tibshirani. A note on the group lasso and a sparse group lasso. *arXiv preprint arXiv:1001.0736*, 2010.
- Alexander J Gibberd and James DB Nelson. Regularized estimation of piecewise constant gaussian graphical models: The group-fused graphical lasso. *Journal of Computational and Graphical Statistics*, 26(3):623–634, 2017.
- Roland Glowinski and A Marroco. Sur l’approximation, par éléments finis d’ordre un, et la résolution, par pénalisation-dualité d’une classe de problèmes de dirichlet non linéaires. *ESAIM: Mathematical Modelling and Numerical Analysis-Modélisation Mathématique et Analyse Numérique*, 9(R2):41–76, 1975.

- Dominique Guillot, Bala Rajaratnam, Benjamin T Rolfs, Arian Maleki, and Ian Wong. Iterative thresholding algorithm for sparse inverse covariance estimation. *arXiv preprint arXiv:1211.2532*, 2012.
- Jian Guo, Elizaveta Levina, George Michailidis, and Ji Zhu. Joint estimation of multiple graphical models. *Biometrika*, 98(1):1–15, 2011.
- David Hallac, Youngsuk Park, Stephen Boyd, and Jure Leskovec. Network inference via the time-varying graphical lasso. In *Proceedings of the 23rd ACM SIGKDD International Conference on Knowledge Discovery and Data Mining*, pages 205–213, 2017.
- Satoshi Hara and Takashi Washio. Learning a common substructure of multiple graphical gaussian models. *Neural Networks*, 38:23–38, 2013.
- Holger Hoefling. A path algorithm for the fused lasso signal approximator. *Journal of Computational and Graphical Statistics*, 19(4):984–1006, 2010.
- Jean Honorio and Dimitris Samaras. Multi-task learning of gaussian graphical models. In *ICML*, 2010.
- Cho-Jui Hsieh, Mátyás A Sustik, Inderjit S Dhillon, and Pradeep Ravikumar. Quic: quadratic approximation for sparse inverse covariance estimation. *J. Mach. Learn. Res.*, 15(1):2911–2947, 2014.
- Nicholas A Johnson. A dynamic programming algorithm for the fused lasso and l0-segmentation. *Journal of Computational and Graphical Statistics*, 22(2):246–260, 2013.
- Steffen L Lauritzen. *Graphical models*, volume 17. Clarendon Press, 1996.
- Hongzhe Li and Jiang Gui. Gradient directed regularization for sparse gaussian concentration graphs, with applications to inference of genetic networks. *Biostatistics*, 7(2):302–317, 2006.
- Zhaosong Lu. Smooth optimization approach for sparse covariance selection. *SIAM Journal on Optimization*, 19(4):1807–1827, 2009.
- Rahul Mazumder and Trevor Hastie. The graphical lasso: New insights and alternatives. *Electronic journal of statistics*, 6:2125, 2012.
- Nicolai Meinshausen, Peter Bühlmann, et al. High-dimensional graphs and variable selection with the lasso. *Annals of statistics*, 34(3):1436–1462, 2006.
- Arkadi Nemirovski. Interior point polynomial time methods in convex programming. *Lecture notes*, 42(16):3215–3224, 2004.
- Yurii Nesterov and Arkadii Nemirovskii. *Interior-point polynomial algorithms in convex programming*. SIAM, 1994.

- Adam J Rothman, Peter J Bickel, Elizaveta Levina, Ji Zhu, et al. Sparse permutation invariant covariance estimation. *Electronic Journal of Statistics*, 2:494–515, 2008.
- Paul Shannon, Andrew Markiel, Owen Ozier, Nitin S Baliga, Jonathan T Wang, Daniel Ramage, Nada Amin, Benno Schwikowski, and Trey Ideker. Cytoscape: a software environment for integrated models of biomolecular interaction networks. *Genome research*, 13(11):2498–2504, 2003.
- Qingming Tang, Chao Yang, Jian Peng, and Jinbo Xu. Exact hybrid covariance thresholding for joint graphical lasso. In *Joint European Conference on Machine Learning and Knowledge Discovery in Databases*, pages 593–607. Springer, 2015.
- Ryan J Tibshirani, Jonathan Taylor, et al. The solution path of the generalized lasso. *The annals of statistics*, 39(3):1335–1371, 2011.
- Quoc Tran-Dinh, Anastasios Kyrillidis, and Volkan Cevher. Composite self-concordant minimization. *J. Mach. Learn. Res.*, 16(1):371–416, 2015.
- Sen Yang, Zhaosong Lu, Xiaotong Shen, Peter Wonka, and Jieping Ye. Fused multiple graphical lasso. *SIAM Journal on Optimization*, 25(2):916–943, 2015.
- Ming Yuan and Yi Lin. Model selection and estimation in regression with grouped variables. *Journal of the Royal Statistical Society: Series B (Statistical Methodology)*, 68(1):49–67, 2006.
- Ming Yuan and Yi Lin. Model selection and estimation in the gaussian graphical model. *Biometrika*, 94(1):19–35, 2007.
- Bai Zhang and Yue Wang. Learning structural changes of gaussian graphical models in controlled experiments. *arXiv preprint arXiv:1203.3532*, 2012.